

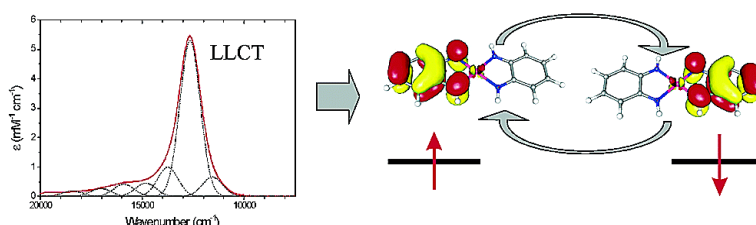
Article

Analysis and Interpretation of Metal-Radical Coupling in a Series of Square Planar Nickel Complexes: Correlated Ab Initio and Density Functional Investigation of [Ni(L)] (L=3,5-di-*tert*-butyl-*o*-diiminobenzosemiquinonate(1-))

Diran Herebian, Karl E. Wieghardt, and Frank Neese

J. Am. Chem. Soc., **2003**, 125 (36), 10997-11005 • DOI: 10.1021/ja030124m • Publication Date (Web): 14 August 2003

Downloaded from <http://pubs.acs.org> on March 29, 2009



More About This Article

Additional resources and features associated with this article are available within the HTML version:

- Supporting Information
- Links to the 34 articles that cite this article, as of the time of this article download
- Access to high resolution figures
- Links to articles and content related to this article
- Copyright permission to reproduce figures and/or text from this article

[View the Full Text HTML](#)



Analysis and Interpretation of Metal-Radical Coupling in a Series of Square Planar Nickel Complexes: Correlated Ab Initio and Density Functional Investigation of $[\text{Ni}(\text{L}^{\text{ISQ}})_2]$ ($\text{L}^{\text{ISQ}}=3,5\text{-di-tert-butyl-o-diiminobenzosemiquinonate(1-)}$)

Diran Herebian, Karl E. Wieghardt, and Frank Neese*

Contribution from the Max Planck Institut für Bioanorganische Chemie, Stiftstr. 34–36, D-45470 Mülheim an der Ruhr, Germany

Received February 19, 2003; E-mail: neese@mpi-muelheim.mpg.de.

Abstract: This paper reports a detailed theoretical study of the interaction between a central low-spin d^8 nickel ion and two *N,N*-coordinating diiminobenzosemiquinonate(1-) ligands in a square planar arrangement. Such complexes have recently attracted much attention due to their unusual bonding patterns, structures, optical, and magnetic properties. Geometry optimizations using various levels of density functional theory (DFT) result in excellent agreement with the experimentally determined structure and in particular reproduce the quinoidal distortions in the aromatic rings well. A detailed analysis of the orbital structure reveals that the complex features essentially two strongly interacting ligand radicals which interact with each other via an efficient superexchange mechanism that is mediated by a back-bonding interaction to the central metal. An analysis of the broken symmetry DFT wave function is presented and a new index for the diradical character is proposed which shows that $[\text{Ni}(\text{L}^{\text{ISQ}})_2]$ has a diradical character of $\sim 77\%$. These results are in full agreement with elaborate multireference post-Hartree–Fock ab initio calculations for $[\text{Ni}(\text{L}^{\text{ISQ}})_2]$ using the difference dedicated configuration interaction (DDCI) method as well as second-order multireference Möller–Plesset (MR-MP2) theory, which give diradical characters of 65–80%. On the basis of these calculations our best estimate for the singlet–triplet gap in this system is 3096 cm^{-1} . This very large value results from an efficient mixing of the ionic configurations into the mainly singlet diradical ground state which is feasible because the semiquinonate SOMOs are delocalized and, therefore, have moderate on-site Coulomb repulsion parameters. As pointed out in the discussion, this represents an interesting difference to the case of magnetically interacting transition metal ions which typically show much smaller magnetic exchange couplings.

1 Introduction

The interaction of transition metal ions with organic radicals is a subject that currently receives much attention.^{1–3} One of the driving forces for this research direction is the realization that such systems exist in the active sites of metalloproteins.² The best understood example is galactose oxidase which features a single Cu(II) ion coordinated to a modified tyrosyl-radical.¹ It is only due to this intricate bonding situation that the enzyme can perform the specific two-electron oxidation of alcohols to aldehydes. Other examples of such electronic structure contributions to reactivity are expected to be found in biochemistry. However, some of them may be difficult to detect in, for example, the cases where there are two radical ligands which strongly couple through a central metal ion. Thus, it is important to have a clear understanding of the bonding and physical properties of such complexes if one wants to understand their

reactivities. Consequently, a large number of transition metal complexes with one-, two-, or three coordinating radicals have been synthesized in recent years and subjected to detailed physical characterization.^{4–10} In many cases, the complexes studied or closely related compounds have been known since the 1960s (see refs 6,7 and references therein). However, it is only recently through a combination of contemporary theory

- (1) (a) Jadzewski, B. A.; Tolman, W. B. *Coord. Chem. Rev.* **2000**, *200*–202, 633. (b) Chaudhuri, P.; Wieghardt, K. *Prog. Inorg. Chem.* **2001**, *50*, 151.
- (2) Sigel, H. S. A. *Metalloenzymes Involving Amino Acid Residue and Related Radicals*; Marcel Dekker: New York, 1994; Stubbe, J.; Van der Donk, W. A. *Chem. Rev.* **1998**, *98*, 705.
- (3) Pierpont, C. G.; Lange, C. W. *Prog. Inorg. Chem.* **1994**, *41*, 331.

- (4) Beckmann, U.; Bill, E.; Weyhermüller, T.; Wieghardt, K. *J. Inorg. Biochem.* **2001**, *86*, 141.
- (5) (a) Chaudhuri, P.; Verani, C. N.; Bill, E.; Bothe, E.; Weyhermüller, T.; Wieghardt, K. *J. Am. Chem. Soc.* **2001**, *123*, 2213. (b) Chun, H. P.; Weyhermüller, T.; Bill, E.; Wieghardt, K. *J. Inorg. Biochem.* **2001**, *86*, 182. (c) Chun, H.; Verani, C. N.; Chaudhuri, P.; Bothe, E.; Bill, E.; Weyhermüller, T.; Wieghardt, K. *Inorg. Chem.* **2001**, *40*, 4157. (d) Chun, H.; Weyhermüller, T.; Bill, E.; Wieghardt, K. *Angew. Chem., Int. Ed. Engl.* **2001**, *40*, 2489. (e) Chun, H.; Bill, E.; Bothe, E.; Weyhermüller, T.; Wieghardt, K. *Inorg. Chem.* **2002**, *41*, 5091. (f) Chun, H. P.; Chaudhuri, P.; Weyhermüller, T.; Wieghardt, K. *Inorg. Chem.* **2002**, *41*, 790. (g) Herebian, D.; Bothe, E.; Bill, E.; Weyhermüller, T.; Wieghardt, K. *J. Am. Chem. Soc.* **2001**, *123*, 10 012. (h) Herebian, D.; Ghosh, P.; Chun, H.; Bothe, E.; Weyhermüller, T.; Wieghardt, K. *Eur. J. Inorg. Chem.* **2002**, 1957.
- (6) (a) Ghosh, P.; Bill, E.; Weyhermüller, T.; Neese, F.; Wieghardt, K. *J. Am. Chem. Soc.* **2003**, *125*, 1293 (b) Neese, F. *J. Phys. Chem. Solids*, **2003**, submitted.
- (7) Herebian, D.; Bothe, E.; Neese, F.; Weyhermüller, T.; Wieghardt, K. E. *J. Am. Chem. Soc.* **2003**, in press.
- (8) Sun, X. R.; Chun, H.; Hildenbrand, K.; Bothe, E.; Weyhermüller, T.; Neese, F.; Wieghardt, K. *Inorg. Chem.* **2002**, *41*, 4295.

and experiment that their properties become understood.^{6,8,10–12} A fascinating case is presented by the neutral complexes of the form $[M(L)_2]$, where L in its formally closed shell form is a dianionic ligand. In a recent paper, Stiefel and co-workers have suggested that complexes of this form containing dithiolene ligands can reversibly and selectively bind olefins which potentially has a large impact on industrial processes.¹³ Interestingly, these dithiolene compounds feature low energy, highly intense absorption bands in the red and near-infrared region of the spectrum which is very similar to the optical spectra that we and others have observed in analogous complexes but without the dithiolene motif. On the basis of extended Hückel calculations, these absorptions have previously been assigned as simple HOMO to LUMO single electron transitions,¹⁴ and the same conclusion was reached in a recent thorough study by Lauterbach and Fabian.¹² However, we felt that this point of view may be an oversimplification and requires a more detailed investigation. In particular, owing to the extremely high absorption coefficients of ϵ up to $10^5 \text{ M}^{-1}\text{cm}^{-1}$ at fairly low energies ($<14\,000 \text{ cm}^{-1}$) these complexes become also interesting for material science in the context of conductivity and nonlinear optical properties.¹⁵

In this paper, we report a detailed model study as well as high-level electronic structure calculations on the prototypical complex $[\text{Ni}(\text{L}^{\text{ISQ}})_2]$, where $(\text{L}^{\text{ISQ}})^{1-}$ represents the *o*-diiminobenzosemiquinonate(1-) π -radical anion, to clarify the electronic information content of the optical spectrum. Our conclusion is that the absorption spectrum carries a large amount of information on the radical–radical coupling in the ground state of these complexes. This is directly related to the diradical character of these systems and, ultimately, also to their reactivities.

2 Materials and Methods

All calculations reported in this paper were performed with the program package ORCA.¹⁶ All geometry optimizations were carried out at the BP86 level^{17,18} of density functional theory except the specifically indicated cases where the B3LYP functional was used.^{17,19} The all-electron Gaussian basis sets used were those reported by the Ahlrichs group.^{20,21} In general, triple- ζ valence basis sets with one set of polarization functions on all non hydrogens were used.²¹ Further

details are found in the Supporting Information (S1). Multireference configuration interaction (MR–CI) calculations were done with a newly developed ORCA module.²² To avoid an overly technical discussion the details of these calculations are documented in the Supporting Information (S2).

Although no symmetry constraints were imposed we will discuss the electronic structure in the D_{2h} point group throughout this paper.

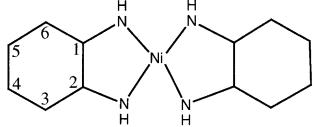
3 Results and Discussion

In this section, we will develop a detailed electronic structure picture of the neutral complex $[\text{Ni}(\text{L}^{\text{ISQ}})_2]$. In the first part, the geometries (section 3.1) and molecular orbitals (MOs, section 3.2) will be discussed. Then a simple model for the ground and excited singlet states will be developed (section 3.3) followed by DFT and correlated ab initio calculations of exchange coupling parameters (section 3.4). Finally, the model developed above will be used to obtain insight into the trends of physical properties observed in the series $[\text{M}(\text{L}^{\text{ISQ}})_2]$ ($\text{M} = \text{Ni}, \text{Pd}, \text{Pt}$) (section 3.5).

3.1 Calculated Geometries. Consistent with the notion that $[\text{Ni}(\text{L}^{\text{ISQ}})_2]$ contains two unpaired electrons the ground-state geometry (vide infra and ref 23) was optimized for the spin triplet state as well as the broken symmetry (BS) state. It turns out that in the case of the BP86 functional, the BS state does not exist and the calculation converges to a closed shell state whereas for the B3LYP functional the BS state exists and is lower in energy than the triplet state (for stability analysis of closed shell wave functions see refs 23,24). This behavior has been observed and analyzed previously.²³ It essentially means that the two methods differ in their estimates of the diradical character of these complexes. A quantitative discussion will be given below on the basis of ab initio CI calculations (section 3.4). From Table 1 it is evident that the optimized structures are in excellent agreement with the experimental findings. The best agreement is observed for the $M_S = 0$ BP86 calculation and, consequently, we base our further calculations on this structure. The slight overestimation of the Ni–N distance is typical of present day DFT functionals. However, the quinoidal distortion in the ring is accurately predicted by the calculations with the typical error in computed bond lengths not exceeding $\sim 0.02 \text{ \AA}$.

3.2 Electronic Structure. More detailed insight into the nature of the magnetic coupling can be obtained by looking at the computed Kohn–Sham MOs but before studying the actual

- (9) (a) Bhattacharya, S.; Gupta, P.; Basuli, F.; Pierpont, C. G. *Inorg. Chem.* **2002**, *41*, 5810. (b) Kaim, W.; Wanner, M.; Knodler, A.; Zalis, S. *Inorg. Chim. Acta* **2002**, *337*, 163. (c) Frantz, S.; Hartmann, H.; Doslik, N.; Wanner, M.; Kaim, W.; Kummerer, H. J.; Denninger, G.; Barra, A. L.; Duboc-Toia, C.; Fiedler, J.; Ciofini, I.; Urban, C.; Kaupp, M. *J. Am. Chem. Soc.* **2002**, *124*, 10 563. (d) Kaim, W.; Dogan, A.; Wanner, M.; Klein, A.; Tiritiris, I.; Schleid, T.; Stufkens, D. J.; Snoeck, T. L.; McInnes, E. J. L.; Fiedler, J.; Zalis, S. *Inorg. Chem.* **2002**, *41*, 4139. (e) Pierpont, C. G. *Inorg. Chem.* **2001**, *40*, 5727. (f) Pierpont, C. G. *Coord. Chem. Rev.* **2001**, *219*, 415; Pierpont, C. G. *Coord. Chem. Rev.* **2001**, *216*, 99. (g) Glockle, M.; Hubler, K.; Kummerer, H. J.; Denninger, G.; Kaim, W. *Inorg. Chem.* **2001**, *40*, 2263. (h) Abakumov, G. A.; Cherkasov, V. K.; Nevodchikov, V. I.; Kuropatov, V. A.; Yee, G. T.; Pierpont, C. G. *Inorg. Chem.* **2001**, *40*, 2434. (i) Pierpont, C. G.; Attia, A. S. *Collect. Czech. Chem. Commun.* **2001**, *66*, 33.
- (10) (a) Lim, B. S.; Fomitchev, D. V.; Holm, R. H. *Inorg. Chem.* **2001**, *40*, 4257. (b) Fomitchev, D. V.; Lim, B. S.; Holm, R. H. *Inorg. Chem.* **2001**, *40*, 645.
- (11) (a) Adams, D. M.; Noodleman, L.; Hendrickson, D. N. *Inorg. Chem.* **1997**, *36*, 3966. (b) Sugiyama, H.; Aharonian, G.; Gambarotta, S.; Yap, G. P. A.; Budzelaar, P. H. M. *J. Am. Chem. Soc.* **2002**, *124*, 12 268. (c) Budzelaar, P. H. M.; de Bruin, B.; Gal, A. W.; Wieghardt, K.; van Lenthe, J. H. *Inorg. Chem.* **2001**, *40*, 4649. (d) Budzelaar, P. H. M.; De Bruin, B.; Gal, A. W.; Van Lenthe, J. H.; Wieghardt, K. *Abstr. Pap. Am. Chem. Soc.* **2001**, *221*, 444. (e) Bencini, A.; Daul, C. A.; Dei, A.; Mariotti, F.; Lee, H.; Shultz, D. A.; Sorace, L. *Inorg. Chem.* **2001**, *40*, 1582. (f) Blomberg, M. A.; Siegbahn, P. E. M. *Mol. Phys.* **1999**, *96*, 571.
- (12) Lauterbach, C.; Fabian, J. *Eur. J. Inorg. Chem.* **1999**, 1995.
- (13) Wang, K.; Stiefel, E. I. *Science* **2001**, *291*, 106.
- (14) Weber, J.; Daul, C.; Van Zelewsky, A.; Goursot, A.; Penigault, E. *Chem. Phys. Lett.* **1982**, *88*, 78.
- (15) (a) Mulder, M. J. J.; Haasnoot, J. G.; Stufkens, D. J.; Tjeng, L. H.; Lin, H. J.; Chen, C. T.; Reedijk, J. *Eur. J. Inorg. Chem.* **2002**, 3083. (b) Kean, C. L.; Miller, D. O.; Pickup, P. G. *J. Mater. Chem.* **2002**, *12*, 2949. (c) Liu, C. M.; Zhang, D. Q.; Song, Y. L.; Zhan, C. L.; Li, Y. L.; Zhu, D. B. *Eur. J. Inorg. Chem.* **2002**, 1591. (d) Robertson, N.; Cronin, L. *Coord. Chem. Rev.* **2002**, *227*, 93. (e) Lacroix, P. G. *Chem. Mater.* **2001**, *13*, 3495. (f) Deplano, P.; Mercuri, M. L.; Pintus, G.; Trogu, E. F. *Comm. Inorg. Chem.* **2001**, *22*, 353. (g) Cocker, T. M.; Bachman, R. E. *Inorg. Chem.* **2001**, *40*, 1550. (h) Kisch, H.; Eisen, B.; Dinnebier, R.; Shankland, K.; David, W. I. F.; Knoch, F. *Chem. Eur. J.* **2001**, *7*, 738.
- (16) Neese, F. *ORCA – an ab initio, Density Functional and Semiempirical Program Package, Version 2.2, revision 41, October 2002* Max Planck Institut für Strahlenchemie, Mülheim, 2002.
- (17) Becke, A. D. *Phys. Rev. A.* **1988**, *38*, 3098.
- (18) Perdew, J. P. *Phys. Rev. B.* **1986**, *33*, 8822.
- (19) Becke, A. D. *J. Chem. Phys.* **1993**, *98*, 5648; Lee, C.; Yang, W.; Parr, R. G. *Phys. Rev. B.* **1988**, *37*, 785.
- (20) Schäfer, A.; Horn, H.; Ahlrichs, R. *J. Chem. Phys.* **1992**, *97*, 2571.
- (21) Schäfer, A.; Huber, C.; Ahlrichs, R. *J. Chem. Phys.* **1994**, *100*, 5829.
- (22) Neese, F. *J. Chem. Phys.*, **2003**, in press.
- (23) Bachler, V.; Olbrich, G.; Neese, F.; Wieghardt, K. *Inorg. Chem.* **2002**, *41*, 4179.
- (24) (a) Bauernschmitt, R.; Ahlrichs, R. *J. Chem. Phys.* **1996**, *104*, 9047. (b) Gräfenstein, J.; Hjerpe, A. M.; Kraka, E.; Cremer, D. *J. Phys. Chem. A* **2000**, *104*, 1748.

Table 1. Calculated Interatomic Distances (in Å) for $[\text{Ni}(\text{L}^{\text{N,N}})_2]$ and the Three Oxidation States of the Free Ligand $\text{L}^{\text{N,N}}$


	$[\text{Ni}(\text{L}^{\text{ISQ}})_2]$ BP86	$[\text{Ni}(\text{L}^{\text{ISQ}})_2]$ BP86	$[\text{Ni}(\text{L}^{\text{ISQ}})_2]$ B3LYP	$(\text{L}^{\text{PDI}})^{2-}$ BP86	$(\text{L}^{\text{ISQ}})^{-}$ BP86	(L^{IBQ}) BP86
exp ^a	$M_S = 1$	$M_S = 0$	$M_S = 0$	$M_S = 0$	$M_S = 1/2$	$M_S = 0$
R(Ni–N)	1.822 ^a	1.871	1.841	1.863		
R(C ₁ –N)	1.350 ^{a*}	1.343	1.350	1.337	1.357	1.329
R(C ₁ –C ₂)	1.429 ^a	1.457	1.446	1.446	1.510	1.504
R(C ₂ –C ₃)	1.425 ^{a*}	1.418	1.416	1.415	1.437	1.446
R(C ₃ –C ₄)	1.383 ^{a*}	1.386	1.386	1.375	1.423	1.387
R(C ₄ –C ₅)	1.423 ^a	1.421	1.419	1.416	1.396	1.417

^a Experimental values for $[\text{Ni}(\text{L}^{\text{ISQ}})_2]$ with *tert*-butyl groups on C₃ and C₅.⁷ Bond distances marked with an asterisk were averaged for comparison to the D_{2h} calculated geometries.

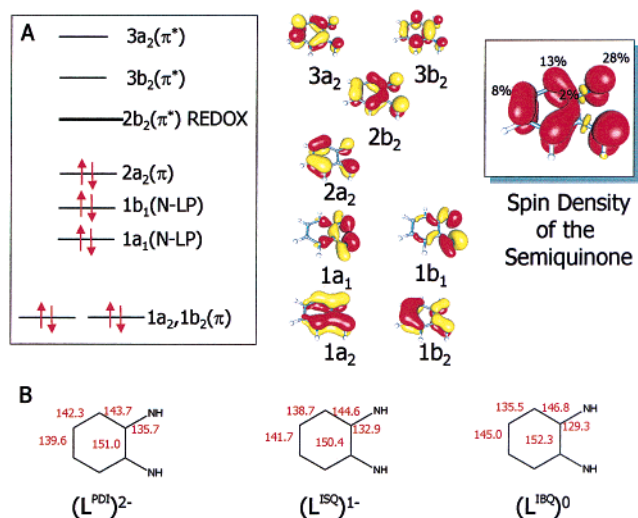


Figure 1. Electronic Structure of the free Ligand $\text{L}^{\text{N,N}}$. (A) The $2b_2$ MO is the redox active MO. It is doubly occupied in the *o*-phenylenediamide(2-) form $(\text{L}^{\text{PDI}})^{2-}$, singly occupied in *o*-diiminobenzosemiquinonate(1-) form $(\text{L}^{\text{ISQ}})^{-}$ and empty in the *o*-diiminobenzoquinone form (L^{IBQ}) . (B) Structural parameters obtained from geometry optimizations on the free ligand (distances in pm).

complex it is instructive to study the electronic structure of the free ligand first (Table 1, Figure 1). As expected, the upper valence region of the $\text{L}^{\text{N,N}}$ ligand features two lone pair orbitals of the nitrogens as well as various π and π^* MOs of the ring system. The redox active MO is dubbed $2b_2$ in Figure 1. It is doubly occupied in $(\text{L}^{\text{PDI}})^{2-}$ (the *o*-phenylenediamide(2-) oxidation level), the singly occupied MO (SOMO) in $(\text{L}^{\text{ISQ}})^{-}$ (the *o*-diiminobenzosemiquinonate(1-) radical anion level) and empty in (L^{IBQ}) (the *o*-diiminobenzoquinone level). Consequently, the spin density in the paramagnetic form $(\text{L}^{\text{ISQ}})^{-}$ clearly reflects the shape of the square of this orbital (Figure 1). The $2b_2$ MO is bonding between C₄ and C₅, antibonding between C₃ and C₄ and also antibonding between the nitrogen and the adjacent carbon atoms. These features are nicely reflected in the calculated geometric distortions upon oxidation from the aromatic form to the quinoidal form of the free ligand. The C₄–C₅ bond significantly expands upon depopulating the $2b_2$ orbital, whereas the C₃–C₄ and C–N bond distances significantly shrink (Table 1, Figure 1).

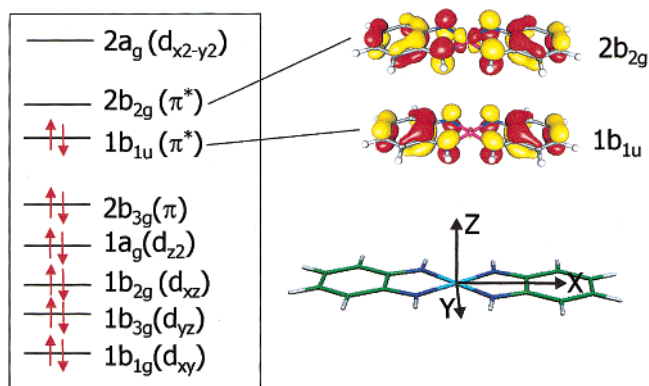


Figure 2. Frontier Orbitals of the Neutral Species $[\text{Ni}(\text{L}^{\text{ISQ}})_2]$ in the closed shell state, the frontier orbitals and the coordinate system chosen.

For the MO description of the neutral complex $[\text{Ni}(\text{L}^{\text{ISQ}})_2]$ within the D_{2h} point group we choose the z -axis to be along the normal of the complex, the x -axis is along the long axis of the complex and the y -axis along the short axis (Figure 2). The MO diagram obtained from the closed shell calculation is shown in Figure 2 and is consistent with the results obtained by Weber et al.¹⁴ It is observed that the upper valence region contains four doubly occupied MOs that are mainly centered on the central Ni ion (not shown). The LUMO+1 orbital is dominated by the Ni $d_{x^2-y^2}$ MO which is strongly σ -antibonding with the ligands (not shown). Thus, the valence state of the Ni is best described as a low-spin d^8 system. Interestingly, the upper valence region also features three π^* MOs of the ligands. The HOMO ($1b_{1u}$) and the LUMO ($2b_{2g}$) correspond especially to the symmetric and antisymmetric combinations of the SOMO of the free benzosemiquinonate(1-) ligand. However, the energetic gap between these two MOs is quite small and amounts to only ~ 1 eV at the BP86 level.²⁵ As a consequence of the small HOMO–LUMO gap, one must expect strong static correlation effects (i.e., “left-right correlation”) and a pronounced diradical character of the system.

For symmetry reasons it is obvious that only the $2b_{2g}$ but not the $1b_{1u}$ ligand fragment orbital can interact with the d -orbitals of the central Ni(II) ion and a Ni- $3d_{xz}$ character of $\sim 15\%$ according to a Löwdin partitioning analysis has been observed in our calculations. Among the simplest models of antiferromagnetic coupling is the model by Hay, Thibault, and Hoffman.²⁶ Their CI model in terms of canonical delocalized orbitals shows that the coupling constant $J(\hat{H}_{HDV} = -2J_{GS}\hat{S}_A\hat{S}_B)$ becomes more negative (antiferromagnetic) as the splitting between the symmetric and antisymmetric combination increases. In the present case, the main reason for the splitting of the two orbitals can be attributed to the interaction of the

(25) Note that orbital energy differences are more meaningful in DFT calculations that do not incorporate the Hartree–Fock exchange compared to those calculated with hybrid functionals or the Hartree–Fock method. In HF calculations the virtual orbitals “see” and N electron system instead of a N-1 electron system as it should be (Szabo, A.; Ostlund, N. S. *Modern Theoretical Chemistry*; MacMillan Pub. Inc.: New York, 1982). Therefore, all of these orbitals are too high in energy and are too diffuse. To the extent that HF exchange is incorporated into hybrid DFT this shortcoming is “inherited” from HF in these functionals. There are no observables that can be meaningfully related to the orbital energy differences in either case. By contrast, for “pure” functionals the virtual orbitals are appropriate and the orbital energy differences are well-defined zero-order approximations for excitation energies (Petersilka, M.; Gossmann, U. J.; Gross, E. K. U. *Phys. Rev. Lett.* **1996**, *76*, 1212; Petersilka, M.; Gross, E. K. U. *Int. J. Quantum Chem.* **1996**, *30*, 181; Görling, A. *Phys. Rev. Lett.* **1996**, *54*, 3912).

(26) Hay, P. J.; Thibault, J. C.; Hoffmann, R. *J. Am. Chem. Soc.* **1975**, *97*, 4884.

ligand b_{2g} combination with the central nickel. Because the combination is antibonding, this interaction raises the energy of the $2b_{2g}$ orbital over the $1b_{1u}$ orbital. Consequently, the superexchange through the central nickel contributes strongly to the observed antiferromagnetism. If one starts the electronic structure description from the situation of a central Ni(II) ion and two benzosemiquinonate(1-) ligands, the metal character in the $2b_{2g}$ MO reflects a metal-to-ligand charge donation and therefore a π -back-bonding interaction. That is, upon one-electron oxidation the $(L^{ISQ})^-$ ligand becomes a fairly good π -acceptor as opposed to its being a strong π -donor in the fully reduced $(L^{PD})^{2-}$ form.

It is clear from the discussion above, that the complex $[Ni(L^{ISQ})_2]$ is best viewed as a central low-spin Ni(II) coordinated by two benzosemiquinonate(1-) type ligands. This means that the single determinant closed shell description is not an appropriate starting point for a quantitative description of the system. Below, such a description both in terms of a simple model as well as on a quantitative level using correlated ab initio electronic structure methods will be developed.

3.3 Configuration Interaction Model of the Ground and Excited States. The intersite interaction between two species with one unpaired electron may be described by a well-known two orbital model.²⁷ This model will be briefly described because it will form the basis for our analysis of the excited states of $[Ni(L^{ISQ})_2]$ as well as of the ground and excited states of the oxidized and reduced species in the forthcoming paper of this series.

The two active MO's ($1b_{1u}$ and $2b_{2g}$) may be written as

$$\psi_{\pm} = \frac{1}{\sqrt{2(1 \pm S)}}(\varphi_a \pm \varphi_b) \quad (1)$$

where φ_a and φ_b are the fragment orbitals on ligands a and b which essentially represent the SOMO's of $(L^{ISQ})^-$ and S is their mutual overlap. It is more convenient to pass to a set of orthogonal localized orbitals $\eta_{a,b} = 2^{-1/2}(\psi_+ \pm \psi_-)$ that are mainly localized on sites a and b but have tails extending to the other side. With two electrons in these two orbitals one can form one triplet and three singlet states. The triplet state and its energy are as follows

$$E(T_0) = -2K_{ab} \quad |T_0\rangle = 2^{-1/2}(|\eta_a\bar{\eta}_b| + |\bar{\eta}_a\eta_b|) \quad (2)$$

where $|\eta_a\bar{\eta}_b|$ is a normalized Slater determinant and a bar over an orbital denotes occupation with a spin-down electron. $K_{ab} = \langle \eta_a\eta_b | r_{12}^{-1} | \eta_a\eta_b \rangle$ is the intersite exchange integral which is intrinsically positive.²⁸ It is usually fairly small and in the present case has been calculated to be $+57 \text{ cm}^{-1}$ by direct integration over the orbitals obtained from a restricted open shell B3LYP calculation. The energies (to second order) and wave functions (exact within the model) describing the three singlet states are as follows

$$E(S_0) \cong -\frac{f_{ab}^2}{J_{aa} - J_{ab}} \quad |S_0\rangle = \cos(\alpha)(|\eta_a\bar{\eta}_b| - |\bar{\eta}_a\eta_b|) + \sin(\alpha)(|\eta_a\bar{\eta}_a| + |\eta_b\bar{\eta}_b|)$$

$$E(S_1) = J_{aa} - J_{ab} - 2K_{ab} \quad |S_1\rangle = 2^{-1/2}(|\eta_a\bar{\eta}_a| - |\eta_b\bar{\eta}_b|) \quad (3)$$

$$E(S_2) \cong J_{aa} - J_{ab} + \frac{f_{ab}^2}{J_{aa} - J_{ab}} \quad |S_2\rangle = -\sin(\alpha)(|\eta_a\bar{\eta}_b| - |\bar{\eta}_a\eta_b|) + \cos(\alpha)(|\eta_a\bar{\eta}_a| + |\eta_b\bar{\eta}_b|) \quad (3)$$

Here, $J_{aa} = \langle \eta_a\eta_a | r_{12}^{-1} | \eta_a\eta_a \rangle = J_{bb}$ is the "on-site" Coulomb repulsion integral, $J_{ab} = \langle \eta_a\eta_a | r_{12}^{-1} | \eta_b\eta_b \rangle$ is the inter-site Coulomb integral which behaves essentially like R_{ab}^{-1} , where R_{ab} is the intercenter distance and f_{ab} is the quasi-one-electron off-diagonal element²⁹ which is often referred to as "transfer" matrix element. The rotation angle α describes the mixing of the "ionic" wave functions with both electrons on the same site into the "neutral" ground state with the two electrons separated. In the closed shell state with ψ_+ doubly occupied $\alpha = \pi/4$ and the ground-state singlet is an equal mixture of ionic and neutral contributions. In the noninteracting limit $\alpha = 0$ and the ground-state singlet is a pure diradical. We therefore define the diradical character as zero for $\alpha = \pi/4$ and 100% for $\alpha = 0$; the diradical index is defined as the percentage neutral character in excess of the closed shell state, i.e., $d \equiv 100(2\cos^2\alpha - 1)$. This definition is preferred over the quantity defined earlier.²³ In the case of an ab initio CI calculation with canonical MOs this definition is identical to

$$d = 200 \sqrt{\frac{c_0^2 c_d^2}{c_0^2 + c_d^2}} \quad (4)$$

where c_0^2 is the weight of the closed shell configuration $(|\psi_+\bar{\psi}_+|)$ in the final CI wave function and c_d^2 is the weight of the double excitation $|\psi_+\bar{\psi}_+| \rightarrow |\psi_-\bar{\psi}_-|$.

3.3.1 Ground State. As is well-known, the ground-state effective exchange parameter from the model above becomes

$$J_{GS} \cong K_{ab} - \frac{2f_{ab}^2}{\Delta J} \quad (5)$$

$(\Delta J = J_{aa} - J_{ab})$. J_{GS} consists of a ferromagnetic part which is given by the "direct" exchange integral (potential exchange) and the second-order antiferromagnetic contribution ("kinetic exchange"). It is also well-known that if one calculates the values for all parameters from ab initio theory the results are poor because the dynamic electron correlation has been neglected.²⁷ This is especially true for the kinetic exchange contribution due to strong electronic relaxation effects in the ionic states.^{27,30,31} In quasidegenerate perturbation theory the effect of the dynamic correlation can be thought of as changing (or "dressing") the parameters up to the point where they reproduce the experimental data.^{27,31} The effective description offered by this simple CI model is therefore still useful.

(27) Calzado, C. J.; Cabrero, J.; Malrieu, J. P.; Caballol, R. *J. Chem. Phys.* **2002**, *116*, 2728.

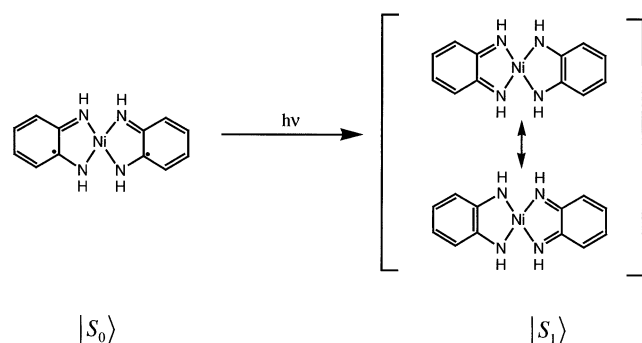
(28) Slater, J. C. *The Quantum Theory of Atomic Structure. Vol II*; McGraw-Hill: New York, 1960.

(29) de Loth, P.; Cassoux, P.; Daudey, J. P.; Malrieu, J. P. *J. Am. Chem. Soc.* **1981**, *103*, 4007.

(30) (a) Fink, K.; Fink, R.; Staemmler, V. *Inorg. Chem.* **1994**, *33*, 6219. (b) Fink, K.; Wang, C.; Staemmler, V. *Int. J. Quantum Chem.* **1997**, *65*, 633. (c) Fink, K.; Wang, C.; Staemmler, V. *Inorg. Chem.* **1999**, *38*, 3847. (d) Kolczewski, C.; Fink, K.; Staemmler, V. *Int. J. Quantum Chem.* **2000**, *76*, 137. (e) Wang, C.; Fink, K.; Staemmler, V. *Chem. Phys.* **1995**, *201*, 87. (f) Wang, C.; Fink, K.; Staemmler, V. *Chem. Phys.* **1995**, *192*, 25.

(31) Calzado, C. J.; Cabrero, J.; Malrieu, J. P.; Caballol, R. *J. Chem. Phys.* **2002**, *116*, 3985.

Scheme 1



3.3.2 Excited States. In an absorption experiment one may observe transitions from $|S_0\rangle$ to $|S_1\rangle$ and $|S_2\rangle$ which occur at energies

$$\Delta_{0-1} \cong \Delta J - 2J_{\text{GS}} \quad (6)$$

$$\Delta_{0-2} \cong \Delta J - 4J_{\text{GS}} - 4K_{ab} \quad (7)$$

The splitting $\Delta_{0-2} - \Delta_{0-1} \approx -2J_{\text{GS}}$, if it could be measured, would provide a direct optical measurement of the ground-state exchange coupling constant (provided that the ferromagnetic term is small compared to J_{GS} as is the case here). However, the transition $|S_0\rangle \rightarrow |S_2\rangle$ is electric dipole forbidden and corresponds to a double excitation in the MO–CI picture. It is therefore unlikely that this transition can be unambiguously identified experimentally. By contrast, the transition $|S_0\rangle \rightarrow |S_1\rangle$ is strongly electric dipole allowed and is readily assigned to the strong near-IR band observed in this class of compounds^{5,7,8} (vide infra). One obtains for the square of the transition dipole moment the approximate relation

$$D_{0-1} \cong R_{ab}^2 \frac{(-2J_{\text{GS}} + 2K_{ab})}{\Delta J} \quad (8)$$

One can safely neglect the ferromagnetic term $2K_{ab}$ in this equation and the conclusion is, therefore, that the intensity of the $|S_0\rangle \rightarrow |S_1\rangle$ transition is directly proportional to the ground state exchange coupling parameter. This transition is essentially a neutral to ionic ligand-to-ligand charge transfer (LLCT) transition³² of the type shown in Scheme 1.

Importantly, this analysis shows that a high energy, high-intensity transition reflects a strong antiferromagnetic exchange interaction in the ground state. Using eqs 6 and 8 and neglecting K_{ab} one can determine the ground-state antiferromagnetic coupling according to

$$J_{\text{GS}} = -\frac{1}{2} \frac{D_{0-1}^2}{D_{0-1}^2 + R_{ab}^2} \Delta_{0-1} \quad (9)$$

and also

$$\Delta J = \frac{R_{ab}^2}{D_{0-1}^2 + R_{ab}^2} \Delta_{0-1} \quad (10)$$

Thus, the experimental determination of the transition energy Δ_{0-1} and the integrated intensity D_{0-1}^2 (vide infra) together with an estimate of the effective intercenter distance R_{ab} will allow an experimental estimate of the ground-state exchange

coupling constant. This will prove to be very useful in the analysis presented below because the exchange coupling constant in $[\text{Ni}(\text{L}^{\text{SQ}})_2]$ and related complexes is so strongly negative that it cannot be measured by any other technique that we are aware of.

It is interesting to compare this situation of metal bridged diradicals with the analogous situation in antiferromagnetically coupled dinuclear transition metal complexes. In dinuclear transition metal complexes the neutral to ionic transition corresponds to the metal-to-metal charge transfer (MMCT)³³ and is so high in energy that it is experimentally not observed. This is due to the large values of the on-site Coulomb repulsion (J_{aa}) which reflect the rather contracted metal d-orbitals. In the case of ligand-ligand magnetic coupling this on-site repulsion is much smaller due to the delocalized nature of the ligand SOMO's and the optical transitions are readily observed. This important fact allows one to extract the model parameters in a straightforward way from the experimental data. This is a new aspect of the present analysis that has to the best of our knowledge not been given before. This simple model is of course closely related to a number of other models that are being used in similar situations of “weak” electronic coupling. For example, it has obvious similarities to the VB–CI model of Tuzcek and Solomon used to explain absorption spectra of antiferromagnetically coupled dinuclear transition metal complexes.^{34,35} The intensity mechanism discussed above is related to the Tanabe-mechanism which has been invoked to explain the intensities spin-forbidden transitions in exchange coupled transition metal dimers.^{35,36} The case of weak interaction in the $(\delta\delta^*)^2$ configuration in metal–metal bonded dimers is similar to the electronic situation discussed here.³⁷ Finally, there is an abundant literature on covalent to ionic excitations in cyclic (L^a versus L^b bands) and open chain (i.e., *trans*-butadiene) conjugated hydrocarbons.

In conclusion, an important outcome of the present analysis is that the assignment of the intense near-IR transition in a large variety of metal dithiolene complexes as the HOMO–LUMO transition^{12,14} is somewhat misleading and the transition should rather be called an LLCT transition. The assignment as a HOMO–LUMO transition would imply that the ground state is well described as a single closed shell determinant with a 1:1 weight of ionic and neutral contributions and a diradical index of zero. On the basis of our analysis this description is not appropriate for the complexes studied here. However, it may be more appropriate for the dithiolene complexes studied by Lauterbach and Fabian¹² because these were found to have

- (32) Vogler, A.; Kunkley, H. *Comm. Inorg. Chem.* **1990**, *9*, 201.
 (33) (a) Anderson, P. W. *Phys. Rev.* **1959**, *115*, 2. (b) Anderson, P. W. In *Magnetism*; Rado, G. T., Suhl, H., Eds.; Academic Press: New York, 1963; Vol. 1, p 25.
 (34) (a) Tuzcek, F.; Solomon, E. I. *Coord. Chem. Rev.* **2001**, *219*, 1075. (b) von Seggern, I.; Tuzcek, F.; Bensch, W. *Inorg. Chem.* **1995**, *34*, 5530. (c) Tuzcek, F.; Bensch, W. *Inorg. Chem.* **1995**, *34*, 1482. (d) Tuzcek, F.; Solomon, E. I. *J. Am. Chem. Soc.* **1994**, *116*, 6916. (e) Solomon, E. I.; Tuzcek, F.; Root, D. E.; Brown, C. A. *Chem. Rev.* **1994**, *94*, 827. (f) Tuzcek, F.; Solomon, E. I. *Inorg. Chem.* **1993**, *32*, 2850. (g) Schenker, R.; Weihe, H.; Güdel, H. U. *Inorg. Chem.* **1999**, *38*, 5593. (h) Schenker, R.; Weihe, H.; Güdel, H. U. *Inorg. Chem.* **2001**, *40*, 4319. (i) Schenker, R.; Weihe, H.; Güdel, H. U.; Kersting, B. *Inorg. Chem.* **2001**, *40*, 3355.
 (35) Schenker, R.; Heer, S.; Güdel, H. U.; Weihe, H. *Inorg. Chem.* **2001**, *40*, 1482.
 (36) (a) Ferguson, J.; Guggenheim, H. J.; Tanabe, Y. *J. Phys. Soc. Jpn.* **1966**, *21*, 692. (b) Ferguson, J.; Guggenheim, H. J.; Tanabe, Y. *J. Chem. Phys.* **1966**, *45*, 1134. (c) Cador, O.; Mathoniere, C.; Kahn, O. *Inorg. Chem.* **2000**, *39*, 3799.
 (37) Miskowski, V. M.; Hopkins, M. D.; Winkler, J. R.; Gray, H. B. In *Inorganic Electronic Structure and Spectroscopy*; Solomon, E. I., Lever, A. B. P., Eds.; John Wiley & Sons Inc.: New York, 1999; Vol. II, p 343.

the smallest diradical index in our previous study.²³ A detailed multiconfigurational ab initio study on the dithiolenes complexes coupled to experimental data appears to be necessary to settle this point. In the present case, we believe that the diradical description is essentially appropriate and that the near-infrared LLCT transition carries a large amount of information about the antiferromagnetic coupling in the ground state of these systems.

3.4 Quantum Chemical Calculations.

3.4.1 Density Functional Calculations. In DFT the dynamic electron correlation is included only implicitly which prevents the direct calculation of the model parameters. Instead, one may optimize a single determinant BS wave function of the type

$$|BS\rangle = |\tau_a \bar{\tau}_b\rangle \quad (11)$$

where τ_a and $\bar{\tau}_b$ are the BS spin-orbitals that are essentially localized on sites a and b, respectively. It is important to realize that these spin-orbitals—in contrast to $\eta_{a,b}$ —are not constrained to be orthogonal by their space parts since their overlap vanishes in the spin integration. In fact, one can start a BS calculation with $\tau_a = \eta_a$ and $\bar{\tau}_b = \bar{\eta}_b$. However, only through the relaxation of $\eta_{a,b}$ to the nonorthogonal $\tau_{a,b}$ pair via the variational principle antiferromagnetism is produced. Importantly, the BS state is, in general, *not* an equal mixture of singlet and triplet states as is frequently assumed. This would only be the case in the noninteracting limit where $\tau_a = \eta_a$ and $\bar{\tau}_b = \bar{\eta}_b$. As discussed in the literature,³⁸ the theoretically most sound way to obtain the exchange coupling parameter in the DFT framework is

$$J_{\text{GS}}^{\text{DFT}} \cong - \frac{E(\text{HS}) - E(\text{BS})}{\langle S^2 \rangle_{\text{HS}} - \langle S^2 \rangle_{\text{BS}}} \quad (12)$$

where $E(\text{HS})$ is the optimized energy of the high-spin (triplet) state, $E(\text{BS})$ the energy of the BS state and $\langle S^2 \rangle_{\text{HS}}$ and $\langle S^2 \rangle_{\text{BS}}$ are the expectation values of the total spin-squared operator for the two calculations. In the case that the spin contamination of the triplet state is negligible this equation can be rewritten

$$J_{\text{GS}}^{\text{DFT}} \cong - \frac{E(\text{HS}) - E(\text{BS})}{1 + \langle \tau_a | \tau_b \rangle} \quad (13)$$

where $\langle \tau_a | \tau_b \rangle \equiv S_{ab}$ is the spatial overlap of the two BS magnetic orbitals. As we have discussed and used previously,⁶ the best way to calculate this overlap integral is through the corresponding orbital method of Amos and Hall³⁹ that allows one to single out the relevant pair of nonorthogonal magnetic orbitals even in many electron systems while all other spin-up and spin-down orbital pairs have a spatial overlap of essentially unity. Thus, the value of S_{ab} is a valid measure of the antiferromagnetism. In the closed shell case, it becomes unity and in the noninteracting case it becomes zero. It is therefore closely related to the diradical index defined above and may be used to calculate it according to

$$d_{\text{DFT}} \approx 100(1 + |S_{ab}|)(1 - |S_{ab}|) \quad (14)$$

As in the CI model above this expression is derived by analyzing the percentage neutral character in the BS wave function in excess of the closed shell state where it equals 50%. It is readily verified that it results in $d_{\text{DFT}} \rightarrow 100$ as $|S_{ab}| \rightarrow 0$ and $d_{\text{DFT}} \rightarrow 0$ as $|S_{ab}| \rightarrow 1$ as required by the reasoning presented above. For $[\text{Ni}(\text{L}^{\text{SQ}})_2]$ we obtain from the B3LYP functional the values $S_{ab} = 0.484$, a sizable $J_{\text{GS}}^{\text{DFT}}$ of -1656 cm^{-1} and a diradical character of $\sim 77\%$. Thus, from the perspective of the B3LYP DFT method, the two radicals are strongly antiferromagnetically coupled and the system has a fairly large diradical character. The computed $J_{\text{GS}}^{\text{DFT}}$ is in good agreement with our earlier results but the diradical index is different owing to the alternative definition used here and which is preferred over the definition used earlier.²³

3.4.2 Ab Initio Calculations. Despite the elegance and efficiency of the BS DFT method it is clear that the wave function associated with the BS state is not satisfactory. The most striking failure of the BS solution is its unphysical spin density (Figure 3). It is observed in this figure that the spin density is large and positive on the left half of the dimer and large and negative on the right half. However, in a genuine singlet state, the spin density has to be precisely zero at every point in space.⁴⁰ It is therefore clear that the BS formalism crudely models the multireference character of these diradical systems but that it is not an entirely satisfactory substitute for a genuine multiconfigurational treatment.

We have therefore explored two multiconfigurational ab initio variants: (a) the difference dedicated CI (DDCI) approach by Caballol, Malrieu, and co-workers⁴¹ (in the two variants DDCI-2 and DDCI-3 discussed in the Supporting Information, S3) and (b) the multireference second-order Möller-Plesset theory (MR-MP2).⁴² As discussed above, the present case requires at least a CAS(2,2) reference with two electrons in two active MOs and this has been used in the DDCI calculations. The MR-MP2 calculations require a larger reference space for accurate results the details of which are discussed and documented in the Supporting Information (S3).

The numbers obtained by the various approaches are collected in Table 2. It is observed that all methods lead to surprisingly consistent predictions of the singlet–triplet gap in $[\text{Ni}(\text{L}^{\text{SQ}})_2]$. Significantly, the correlated ab initio methods predict splittings that are very close to the BS-B3LYP predictions which lends further support to the analysis given above. The DDCI-2 number is significantly smaller than the other values. However, based on the insights provided by Malrieu and co-workers this is simply the expected behavior due to the neglected dynamic repolarization contributions as analyzed in detail by Calzado

- (38) Soda, T.; Kitagawa, Y.; Onishi, T.; Takano, Y.; Shigetani, Y.; Nagao, H.; Yoshioka, Y.; Yamaguchi, K. *Chem. Phys. Lett.* **2000**, *319*, 223, and references therein.
 (39) (a) Amos, A. T.; Hall, G. G. *Proc. R. Soc. Ser. A* **1961**, *263*, 483. (b) King, H. F.; Stanton, R. E.; Kim, H.; Wyatt, R. E.; Parr, R. G. *J. Chem. Phys.* **1967**, *47*, 1936.

- (40) McWeeny, R. *Methods of Molecular Quantum Mechanics*; Academic Press: London, 1992.
 (41) (a) Miralles, J.; Caballol, R.; Malrieu, J. P. *Chem. Phys.* **1991**, *153*, 25. (b) Miralles, J.; Daudey, J. P.; Caballol, R. *Chem. Phys. Lett.* **1992**, *198*, 555. (c) Miralles, J.; Castell, O.; Caballol, R.; Malrieu, J. P. *Chem. Phys. Lett.* **1993**, *172*, 33. (d) Cabrero, J.; Caballol, R.; Malrieu, J. P. *Mol. Phys.* **2002**, *100*, 919. (e) Ilas, F.; Moreira, I. P. R.; de Graaf, C.; Barone, V. *Theor. Chem. Acc.* **2000**, *104*, 265.
 (42) (a) Wolinski, K.; Pulay, P. *J. Chem. Phys.* **1989**, *90*, 3647. (b) Andersson, K.; Malmqvist, P. A.; Roos, B. O.; Sadlej, A. J.; Wolinski, K. *J. Phys. Chem.* **1990**, *94*, 5483. (c) Andersson, K.; Malmqvist, P. A.; Roos, B. O. *J. Chem. Phys.* **1992**, *96*, 1218. (d) Andersson, K. *Theor. Chim. Acta* **1995**, *91*, 31. (e) Murphy, R. B.; Messmer, R. P. *Chem. Phys. Lett.* **1991**, *183*, 443. (f) Hirao, K. *Chem. Phys. Lett.* **1992**, *190*, 374. (g) Nakano, H. *J. Chem. Phys.* **1993**, *99*, 7983. (h) Grimme, S.; Waletzke, M. *Phys. Chem. Chem. Phys.* **2000**, *2*, 2075

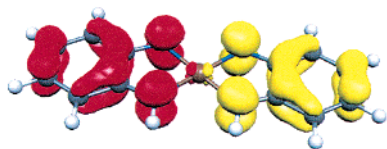


Figure 3. Total spin density of $[\text{Ni}(\text{L}^{\text{ISO}})_2]$ from a BS B3LYP calculation.

Table 2. Exchange Coupling Constants and Diradical Character in $[\text{Ni}(\text{L}^{\text{ISO}})_2]$ as Predicted by Various DFT and Correlated ab Initio Methods

method	$-2J_{\text{GS}}$ (cm^{-1})	% diradical ^a
B3LYP	3312	77
DDCI-2	1545	80
DDCI-3	3096	65
MR-MP2[g0]	4004	79
MR-MP2[g3]	3698	79

^a For DFT calculated with eq 14 and with eq 4 for the ab initio calculations. All ab initio values have been obtained with open-shell triplet state Hartree–Fock MOs.

and Malrieu in a recent series of papers.^{27,31,43} In addition, it has been observed that the numbers obtained with the DDCI methodology are stable and only depend to a minor extent on the orbitals used for the calculation (i.e., closed shell Hartree–Fock orbitals, triplet ROHF orbitals or Kohn–Sham orbitals). On the other hand, the predictions by the MR-MP2 method are fairly sensitive to the details of the construction of the reference space, the orbitals used and the definition of the 0th order Hamiltonian. Although we have already used fairly large reference spaces with up to 24 active electrons and 27 active MOs the results are still not completely converged and changes of the order of $\sim \pm 500 \text{ cm}^{-1}$ in the singlet–triplet gap are within the uncertainties of the present MR-MP2 calculations.

Nevertheless, all theoretical methods lead to the consistent prediction of the singlet–triplet gap on the order of magnitude of $\sim 3000\text{--}4000 \text{ cm}^{-1}$ which is fairly large. For the following we accept the DDCI-3 value of 3096 cm^{-1} as our best theoretical estimate. Importantly, all methods predict a significant diradical character in $[\text{Ni}(\text{L}^{\text{ISO}})_2]$ which varies between 65% and 80% depending on the theoretical method. Since the percentage diradical character is not an observable a discussion about the best value might be academic. It is, however, significant that all correlated ab initio methods find a large diradical character.

3.5 Analysis of Experimental Data. The experimental absorption spectrum of $[\text{Ni}(\text{L}^{\text{ISO}})_2]$ between 5000 and 25 000 cm^{-1} together with a Gaussian fit is shown in Figure 4 and Table 3. It is evident that more than one absorption band is required to fit the experimental spectrum. However, the spectrum is strongly dominated by the intense transition centered at 12 660 cm^{-1} which is assigned to the LLCT transition.⁷

LLCT State. The extinction coefficient for the LLCT transition is $\sim 54\,000 \text{ M}^{-1} \text{ cm}^{-1}$.⁷ According to the Gaussian fit this corresponds to a very large oscillator strength of $f_{\text{exp}} = 0.287$ which is calculated from

$$f_{\text{exp}} = 4.32 \times 10^{-9} \int \epsilon(\nu) d\nu \quad (15)$$

with ϵ being the extinction coefficient ($\text{M}^{-1} \text{ cm}^{-1}$) and ν the

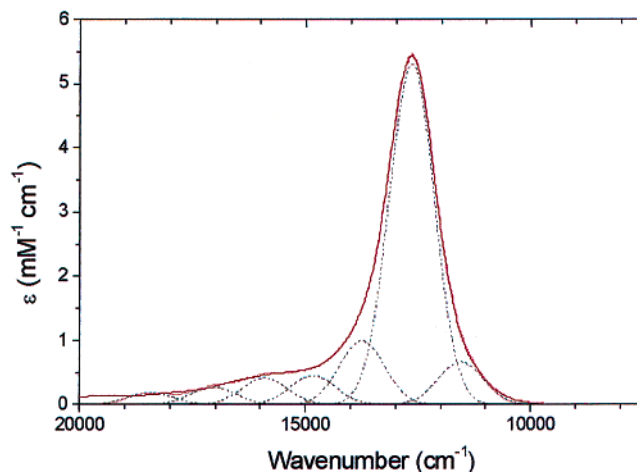


Figure 4. Experimental absorption spectrum of $[\text{Ni}(\text{L}^{\text{ISO}})_2]$ in acetonitrile and Gaussian resolution using the parameters in Table 3.

Table 3. Gaussian Fit Parameters for the Absorption Spectrum of $[\text{Ni}(\text{L}^{\text{ISO}})_2]$ in Figure 4

position (cm^{-1})	$f_{\text{GSC}} \times 10^4$
11 550	36
12 660	287
13 740	54
14 830	24
15 900	15

photon energy measured in cm^{-1} . Alternatively, the oscillator strength may be calculated from

$$f_{\text{exp}} = 3.04249 \times 10^{-6} \bar{\nu} D_{\text{exp}}^2 \quad (16)$$

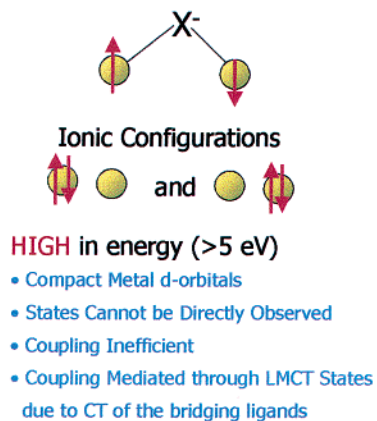
where $\bar{\nu}$ is the vertical transition energy (assumed to coincide with the band maximum here) and D_{exp}^2 is the square of the transition dipole moment in atomic units. Thus, the experimental estimate of the transition dipole moment is

$$D_{\text{exp}}^2 = 0.001420 \frac{\int \epsilon(\nu) d\nu}{\bar{\nu}} \quad (17)$$

which amounts to 7.45 au^2 for $[\text{Ni}(\text{L}^{\text{ISO}})_2]$ in acetonitrile. If we would have an accurate value for R_{ab} one could now evaluate eq 9 to get a purely experimental estimate of the ground state exchange coupling. However, since it is difficult to unambiguously arrive at an estimate of R_{ab} we will fix this value with reference to our most accurate ab initio result for $-2J_{\text{GS}} = 3096 \text{ cm}^{-1}$ which results in $R_{ab} \approx 5 \text{ au}$ or an effective electron-transfer distance of $\sim 2.5 \text{ \AA}$. If one makes the plausible assumption that this number is transferable between complexes of similar chemical constitution, then one can use eq 9 to arrive at an estimate of the exchange parameter for related complexes.⁴⁴ Using the spectral data obtained in acetonitrile⁷ we find for $[\text{Pd}(\text{L}^{\text{ISO}})_2]$ $D_{\text{exp}}^2 = 6.03 \text{ au}^2$, $\Delta_{0 \rightarrow 1} = 12690 \text{ cm}^{-1}$ and $-2J_{\text{GS}} = 2634 \text{ cm}^{-1}$, whereas for $[\text{Pt}(\text{L}^{\text{ISO}})_2]$ the parameters $D_{\text{exp}}^2 = 7.98 \text{ au}^2$, $\Delta_{0 \rightarrow 1} = 13\,986 \text{ cm}^{-1}$ and $-2J_{\text{GS}} = 3600 \text{ cm}^{-1}$ are obtained. These results suggest that the interaction through the central palladium are slightly weaker than through the central nickel, whereas the interaction through the central platinum(II) is the strongest in the series. The latter case also nicely illustrates the trend of increasing intensity with increasing transition energy of the LLCT transition which is predicted by the model.

(43) (a) Calzado, C. J.; Sanz, J. F.; Malrieu, J. P.; Ilas, F. *Chem. Phys. Lett.* **1999**, *307*, 102. (b) Calzado, C. J.; Malrieu, J. P. *Chem. Phys. Lett.* **2000**, *317*, 404. (c) Calzado, C. J.; Sanz, J. F.; Malrieu, J. P. *J. Chem. Phys.* **2000**, *112*, 5158.

Transition Metal Dimers



Metal Bridged Diradicals

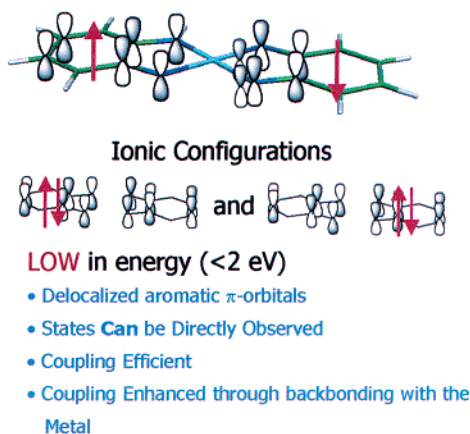


Figure 5. Comparison of antiferromagnetic coupling mechanisms in bridged dimetallic complexes compared to metal bridged diradicals.

Previously Lauterbach and Fabian have predicted the higher energy of the LLCT transition to arise from the relativistic bond contraction present for the heavy central Pt(II) which leads to more efficient orbital overlap.¹² This point of view is consistent with our interpretation and nicely explains why the [Pt(L^{ISQ})₂] is more strongly antiferromagnetically coupled than [Ni(L^{ISQ})₂].⁴⁵

4 Conclusions

The present work has led to a detailed quantitative description of the electronic structure of the neutral complexes [Ni(L^{ISQ})₂]. However, the results reported here have a much broader range of applicability. Thus, the conclusions carry over with limited changes to other d⁸ metals such as Pd(II) and Pt(II) or to complexes where the amide nitrogens are replaced with appropriate oxygen or sulfur donors. A number of such complexes have been reported previously.^{4,5,8} The model developed here will apply to all of these complexes and perhaps also to other highly interesting compounds such as transition metal dithiolenes which are of biological relevance.

The analysis presented above shows that the complexes of this series are best described as strongly exchange coupled diradicals (diradical index ~65–80%) which interact through a diamagnetic central M(II) ion in a low-spin d⁸ configuration. The key results of the analysis may be summarized as follows: (1) Back-bonding between the metal and the benzosemi-

quinonate(1-) ligand enhances the strong exchange coupling through efficient superexchange involving the metal d_π-orbitals. In chemical terms, the benzosemiquinonate(1-) becomes a strong π -acceptor in sharp contrast to the strongly π -donating character of the dianionic *o*-phenyldiamide(2-) form of the ligand. (2) The low energy of the ionic ligand-to-ligand charge transfer configurations leads to efficient mixing with the neutral ground state and consequently to a high diradical index and a large exchange coupling constant. (3) The intensity of the LLCT transition is directly proportional to the Heisenberg exchange coupling parameter in the ground state. As discussed above, the model outlined in this work has similarities with other models that apply to situations of “weak” interelectronic coupling such as the VB–CI model,^{34,35} the electronic structure of the ($\delta\delta^*$)² configuration in metal–metal bonded systems³⁷ or the Tanabe intensity mechanism in exchange coupled transition metal dimers.^{35,36}

In addition to these qualitative insights, we have reported detailed DFT and ab initio investigations of the singlet–triplet gap because it is too large to be accurately measured experimentally. Through the model developed in this paper together with a single parameter which has been determined from our most accurate ab initio result one can use the position and the intensity of the highly intense near-IR band to obtain an estimate of the ground state exchange coupling parameter. The results for a series of related complexes predict the Pt(II) ion to mediate a stronger exchange coupling between the radical ions compared to the central Ni(II) complex while Pd(II) behaves similar to Ni(II) albeit gives a slightly weaker coupling.

It is instructive to compare the electronic situation discussed in this paper with the one commonly found in dinuclear transition metal complexes with interacting paramagnetic ions (Figure 5). In these complexes the popular Anderson model attributes the antiferromagnetic contributions to the mixing of ionic metal-to-metal charge transfer (MMCT) states into the neutral ground state. However, these MMCT states are high in energy and fall deep into the UV region of the spectrum which usually precludes their experimental analysis. The origin of the high energy of these states is that the donor and acceptor orbitals are rather compact metal d orbitals. Thus, the increase in electron–electron repulsion by moving an electron from one-metal to the other must amount to several electronvolts. This

(44) The additional absorption bands seen in the experimental spectrum are assigned to d–d transitions of the central low-spin Ni(II) ion. Although we have undertaken some preliminary ab initio calculations of the complete spectrum, it became evident that the electronic structure of the additional excited states is exceedingly complex. This is due to complicated spin-coupling situations in the d–d-excited states. The central Ni(II) has a closed shell configuration in the ground state but has two unpaired electrons in d–d singly excited states. These two electrons can either couple to a singlet or a triplet. In addition, the two unpaired electrons on the ligand can also be coupled to give singlets and triplets. In the case where both, the central Ni(II) and the ligand-diradical exist in triplet states these can couple to give an overall singlet excited state. In keeping with Gouterman’s nomenclature, these transitions may be characterized as trip-singlets (Cory, M. G.; Zerner, M. C. *Chem. Rev.* **1991**, *91*, 813). Although these excited states are not expected to have intensity on their own they can readily mix with the intense LLCT band to gain some intensity and since the intensities of the additional transitions are decreasing with increasing energetic separation from the LLCT band it is reasonable to expect this to be one of the main intensity mechanisms.

(45) For simplicity one may assume a constant band shape for the LLCT transition and estimate the transition dipole moment from the value found for [Ni(L^{ISQ})₂] as $D_{\text{exp}}^2 \cong 7.45 \times (\epsilon_{\text{max}}/54\,000)$, where ϵ_{max} is the extinction coefficient of the unknown species at the band maximum.

high energy also means that the antiferromagnetic interaction mediated by this mechanism cannot be highly effective which is consistent with the observed exchange coupling constants in transition metal dimers which rarely exceed a few hundred wavenumbers.

The situation is completely different for the case of the metal bridged diradicals studied here. In this case the donor and acceptor orbitals are rather delocalized π^* orbitals. Consequently, the increase in electron–electron repulsion in the ionic states is much smaller and the LLCT fall into the visible and near-infrared region of the spectrum. This allows a detailed experimental characterization of these states and a large amount of information can be extracted from a study of the optical properties of such systems. The principal information content has been developed in this paper, and we are currently studying the optical spectra of a number of such complexes in order to more quantitatively define the trends in antiferromagnetic coupling as mediated by different ligands and metal ions.

Based on the basic description of the electronic structure of $[\text{Ni}(\text{L}^{\text{SQ}})_2]$ developed here one can also obtain a detailed understanding of the oxidized and reduced species of the form $[\text{M}(\text{L}^{\text{X,Y}})_2]^{2-,1-,1+,2+}$ ($\text{M} = \text{Ni, Pd, Pt}$, $\text{X, Y} = \text{NR}^-, \text{S}^-, \text{O}^-$). The detailed analysis of the electronic structure and physical

properties of this series of compounds will be the subject of the next paper in this series.

Finally, the diradical character of the neutral complexes studied here should be related to the reactivity of these complexes. It may be expected that a higher amount of effectively unpaired electrons is related to a more pronounced ability of the ligands to support radical reactions. Because the diradical character increases with decreasing coupling one has now a handle to experimentally and theoretically evaluate such a proposal. In future work, we plan to pursue the relation between the spectral and reactivity properties of these systems in detail—experimentally as well as theoretically.

Acknowledgment. We gratefully acknowledge helpful discussions with Drs. Bachler and van Gestel. The development of ab initio methods for open-shell systems is financially supported within the DFG priority program “Molecular Magnetism” which is gratefully acknowledged.

Supporting Information Available: Details of DFT and ab initio calculations (5 pages, print/PDF). This material is available free of charge via the Internet at <http://pubs.acs.org>.

JA030124M